THERMAL-HYDRODYNAMIC MODELING OF LABORATORY TESTS ON THE INTERACTION OF $NaNO_3$–NaOH FLUIDS WITH SANDSTONE ROCK AT A DEEP RADIONUCLIDE REPOSITORY SITE

A.V. Kiryukhin[1], E.P. Kaymin[2], and E.V. Zakharova[2]

[1]Institute Volcanology and Seismology FEB RAS, Piip-9, P-Kamchatsky, Russia 683006

[2]Institute of Physical Chemistry and Electrochemistry RAS, Leninsky-31, Moscow, Russia, 119991

e-mail: avk2@kscnet.ru

ABSTRACT

Thermal-hydrodynamic modeling was used to reproduce laboratory tests involving sandstone samples collected from a deep radionuclide repository site at the Siberia Chemical Plant, Seversk (Russia). Laboratory tests included injection of alkaline fluids into sandstone samples at 70°C. Some minerals were constrained in the model to precipitate or dissolve, according to laboratory test results. Modeling results were compared with observed test data (mineral phase changes, transient concentration data at the outlet of a sample column). Reasonable agreement was obtained between calculated and measured mineral phases (Na-smectite and kaolinite precipitation, quartz, microcline, chlorite, and muscovite dissolution). After cation exchange option used in the model, the most abundant secondary mineral generated was dawsonite, which correspond to sodium carbonates observed in the sample after injection test. Time dependent chemical concentrations (transient chemical concentration data) at the outlet of sample column qualitatively matched to the data observed.

INTRODUCTION

Deep injection (at 314-341 m below surface) of liquid radioactive waste, conducted in Russia at radiochemical plants sites over the last 40 years, was considered a reliable method of isolating such waste from the ecosphere. Aquifer reservoir rock behaves as a natural absorber of polluted injection flow under deep-repository site environmental conditions. Nevertheless, such

repository sites are considered a potential source of environmental pollution. In light of this, safety criteria are have been developed to characterize different critical situations and to take adequate preventive measures [1]. One such criterion is the restriction of temperature rise caused by radiogenic heat release from nuclear waste components, with upper-temperature limits considered to be below saturation temperature under specific aquifer conditions. For existing deep-injection repository sites, the upper temperature limit is estimated to be 150–180^{o}C due to the radioactive decay of waste components. Measures to maintain temperatures below upper limit achieved by reducing radionuclides injection rate during exploitation, modeling heat-transfer processes in deep repository site are carried out too [2]. When liquid radionuclide waste was injected into layer-type reservoirs (Siberia Chemical Plant (SCP), Seversk; Mining Chemical Plant (MCP), Zheleznogorsk), chemical interaction took place between natural pore fluids and the clay minerals of the repository site. New secondary minerals were created, initial minerals dissolved, and temperature increased as a result of radiogenic heat release [3]. Chemical interactions between injected fluids and the clay-sandstone minerals in the aquifer rock were intensified by high temperature and pressure conditions, conditions that could affect the transport parameters of radioactive components. Monitoring of the hydrogeological parameters in the observational wells, as well as laboratory injection experiments under a specified range of pressure, temperature and physical-chemical conditions, were used to obtain reliable information on underground repository processes [4, 5].

However, in addition to all this work, reliable numerical models were needed to forecast deep-injection process parameters, and to determine injection rates and experimental schedules under safe thermal-hydrodynamic requirements. For this modeling effort, we used TOUGHREACT V1.0, a computer code designed to simulate thermal-hydrodynamic-chemical (THC) processes, including multiphase nonisothermal transport and fluid-rock chemical-reaction kinetics [6]. In other studies involving TOUGHREACT, fluid chemical interaction had been successfully implemented reproducing THC processes and the associated secondary minerals

observed in some geothermal fields within regions of recent volcanic activity [7, 8]. Similar processes have taken place during radionuclide-waste fluid injection in sandstones aquifers, including dissolution of primary minerals and generation of secondary minerals as a result of kinetically driven chemical reactions between rocks, initial fluids and injected fluids. Hence, in this study, we sought to verify TOUGHREACT's ability to numerically reproduce laboratory tests to the process of technogenic alteration observed in sandstone samples (obtained from the Siberia Chemical Plant deep repository site) as a result of chemical interaction during $NaNO_3$–NaOH fluid injection in rock samples at a temperature of 70^{o}C (temperature measured by well logging in repository aquifer). (These laboratory tests were performed at the Institute of Physical Chemistry RAS). Modeling results were calibrated against observed secondary minerals generated during the laboratory experiment and identified based on microprobe analysis, and against the transient chemistry data of fluids discharged from the core outlet during the experiment. The aim of the model calibration was: 1. Analyze the possibility to generate in the model the same set of precipitated and dissolved minerals, as observed in the laboratory experiment, 2. Analyze the possibility to reproduce in the model transient chemical concentrations of fluids discharged from the core outlet.

LABORATORY EXPERIMENT CONDITIONS

Initial Mineral Composition of Rock Sample

The initial rock sample from the Siberia Chemical Plant deep-repository site is composed of quartz-feldspar sandstone. The dominant feldspars are potassium feldspar (Kfs) and sodium feldspar - albite (Ab), with sodium-potassium feldspar (Fsp) is very rarely observed. Significant fractions of kaolinite (Kaol), montmorillonite (Mont), micas, and chlorite are also observed. Montmorillonite forms large aggregates and surrounds around other minerals. Initial rock samples are characterized by some alteration: specifically, feldspars, micas, and chlorite have been partially replaced by montmorillonite, while muscovite is sometimes replaced by kaolinite.

Laboratory Test Performance

To conduct laboratory experiments in conditions relevant to deep repository site of the fluid-rock chemical interaction under high temperature and pressure flows, the following testing facility was design (Figure 1).

High pressure vessel – rock sample site (1) with interior diameter 32 mm and exterior diameter 90 mm was made from thermal resistant alloy. Screw press (2) connected to high pressure vessel (1) through triple valve (3) used to support pressure into rock sample. Pressure gauges (7 and 8, upper limit 160 MPa, 0.4% accuracy) used to monitor flow conditions. Infiltration solution fluid located in separator (12). Gas pressure from vessel (9) drive out solution into rock sample site. Then solution enter triple valve (16) and through valve (17) collected in vessel (18). Sample input and output pressures are monitored by gauges (11 and 19, upper limit 60 MPa, 0.25% accuracy). Pressure monitoring data transmitted into registration block (27) and recorded by PC (28). Temperature maintained by electrical heater (23) combined with temperature regulator 9TYP 014T (25). To monitor temperature conditions Cr-Al thermocouple used (21 and 22). Thermocouples connected through cold alloy thermostat (24). Temperature records conducted through registration block (27) by PC (28), total temperatures measurements accuracy $\pm 3^{o}C$. All joints are made from acid- and alkaline-solutions resisted materials.

Rock sample preparation include distraction of original sandstone sample into small cuts (it was not possible to make a cylinder from core sample) and loaded into tube sample site. It worth to note specific surface area of the crushed and uncrushed samples was estimated using QUANTASORB method in the range of 12.8 m^2/g - 12.2 m^2/g, while gas-estimated permeability's for 4-sm cubic samples ranges from 21.8 mD (vertical) to 85.7 mD (horizontal). The total porosity of sandstones was estimated as 20% based on values of specific densities of rocks and mineral grains [9].

Before testing, rock sample installed in a tube form with diameter of 15 mm and length 120 mm, isolated by thermo-relax able rubber. Laboratory test run started by pushing solution through valve (3) and gauges set (5 and 6) by press (2) into high pressure vessel - sample site (1).

Test pressure fit accordingly to lithostatic pressure of sampling depth, taking in account sandstones density 2 g/sm^3 [3]. Test temperature fit by temperature regulator (25), accordingly to observed temperatures in deep repository site. Then gas from vessel (9) is pushing into separator (12) and fluid system is fill up to desired fluid pressure. After 3-5 hours desired flow rate regime achieved. Constant flow rate maintained by adjusting of the input (13) and output (17) valves and defined volumetrically (vessel 18).

Chemical composition of rock sample converted into mineralogical composition based on Selector-C computer code [4]. Hence, mineralogical composition (as listed in Table 1) includes (in weight %): quartz (55–65), feldspars (albite, plagioclase, microcline) (10–20), micas (2–10), chlorite (up to 2), clay minerals (montmorillonite, kaolinite) (up to 15), and carbonates of calcium and magnesium (0.5–3.0%). The initial fluid chemical composition corresponds to pore fluids at the deep repository site (Table 3). An alkaline solution was injected into the column at 3 MPa pressure and 70^{o}C temperature. This solution included the following components (in g/L): $NaNO_3$—44.3, Na_2CO_3—2.08, Al—0.83, NaOH—8.9 (Table 3). There was no direct pH measurements of injected solutions during laboratory experiment, hence thermodynamic software (Selector, Gibbs) used for pH estimations based on input concentrations mentioned above (Table 3). GIBBS supported thermodynamic database UNITHERM is consistent with EQ3/6 database TOUGHREACT used.

Two tests having durations of 79 days and 42 days were performed, with injection mass flux at an average level of 2.50×10^{-5} kg/s m^2. At various times during the test (9, 16, 23, 30, 32, 58, and 79 days), the alkaline fluid was sampled at the column outlet for chemical analysis (Na, Al, Si, Ca, Mg, K, and Sr) (Table 4).

After the tests, microprobe analyses of the samples mineral compositions were performed [10, 11], via the connection of Link INCA ENERGY200 to an electronic scan facility, CamScan MV-2300**,** Energy Dispersive Spectroscopy (EDS) techniques used (Figure 2). Findings were as follows: (1) biotite, chlorite, and feldspars were replaced by Na-smectites, (2)

muscovite was replaced by kaolinite, (3) Na-smectite precipitation was greater then kaolinite precipitation, (4) siderite was not significantly changed, (5) magnetite precipitated, (6) sodium carbonate precipitate ($Na_2CO_3 \times 10H_2O$ (or trona $Na_3H(CO_3)_2 \times 2H_2O$) was found in the inflow zone, and (7) increasing the test duration did not cause an increase in the degree of hydrothermal alteration within the sandstone sample column. This last finding indicates that secondary minerals formed a cover, isolating other minerals from participation in chemical reactions.

NUMERICAL THERMAL-HYDRODYNAMIC-CHEMICAL MODEL SETUP

In this study, TOUGHREACT V1.0 was used to reproduce the laboratory experiment just described: the process of technogenic alteration observed in sandstone. The model accounts for adjective and diffusive transport of aqueous chemical species. Mineral dissolution/precipitation can proceed at equilibrium and/or under kinetic conditions, according to the following rate law:

$$r = kS\,(1-Q/K)\exp(E_a/(R*298.15)-E_a/(RT)) \quad (1)$$

where k is the kinetic constant of the chemical dissolution/precipitation at 25 ^oC, mole/s·m^2; S is the specific reactive surface area, m^2/m^3; Q is the activity product; K is the equilibrium constant for mineral-water interaction; E_a is the activation energy, kJ/kmole; R is the gas constant, kJ/kmole K, and T is temperature, in K. Temperature effects are also accounted for in TOUGHREACT by geochemical-reaction calculations, in which equilibrium and kinetic data are functions of temperature.

Chemical Input Data

Quartz, microcline, albite-low, Na-smectite, kaolinite, chlorite, muscovite, and sodium carbonates (nitrite, trona or dawsonite) were used for geochemical system definition, initial mineral fractions and chemical interaction parameters were assigned as shown in Tables 1 and 2.

Dawsonite $NaAlCO_3(OH)_2$ was add into EQ3/6 database TOUGHREACT used. This reasoned by dawsonite precipitation trigger aluminum consume from injecting fluids, which not seen in the fluid exiting the column. For the reaction $NaAlCO_3(OH)_2 + 3H^+ = Na^+ + Al^{3+} + HCO_3^- + 2\,H_2O$

corresponding log K = 2.1 at 70^{o}C used according to our paper unknown Reviewer comment, which was converted for reaction $NaAlCO_3(OH)_2 = 3H^+ + Na^+ + AlO_2^- + HCO_3^-$ to log K = -16.7 using TOUGHREACT kreg and switch utility's for geochemical system based on AlO_2^- primary specious.

Energy of activation E_a parameter was assigned as in (Table 3, [7]), while others (*k* and S) were changed during model calibration. Its worth to note, that rate law formulae (1) include multiplication of kinetic constant *k* and specific reactive surface area S, and individual change of those parameters have no effect on model output, if their multiplication product have no change. Hence *k*S used as a calibration parameter to fit model output to observation data. As initial approach for *k* and S - data derived from (Table 3, [7]) used. The chemical composition (primary species) of the initial solution (natural pore fluids) and injected fluid are shown in Table 3. In addition the following list of aqueous complexes used: OH^-, $HAlO_2(aq)$, $NaAlO_2(aq)$, $CaSO_4(aq)$, $NaCl(aq)$, $CaHCO_3^+$, $CO_2(aq)$, CO_3^{-2}, $CaCO_3(aq)$, $KCl(aq)$, $NaSO_4^-$, KSO_4^-, $NaHSIO_3(aq)$, $CaOH^+$, $NaOH(aq)$, $H_3SIO_4^-$, Al^{+3}, $AlOH^{+2}$, $Al(OH)_2^+$, $Al(OH)_3(aq)$, $CaCl^+$, $CaCl_2(aq)$, $NaHCO_3(aq)$, $MgHCO_3^+$, $MgCl^+$, $MgSO_4(aq)$, $NaCO_3^-$, $FeCl^+$, $FeHCO_3^+$, $FeCO_3(aq)$, $FeCl_4^{-2}$.

Flow and Solute Input Data

In adherence to the laboratory test data, the model was assigned a 70 ^{o}C isothermal condition with mass flux 2.50×10^{-5} kg/s m^2 and pressure 3.0 MPa. Reservoir porosity was assigned to be 0.2. The length of the model corresponded to the length of test sample, 15 cm. A 1-D numerical grid was generated that included 32 elements, with B 1 representing the source of injected fluid (specified as inactive element with large volume $5.00E^{+20}$ m^3); R1–R30 elements representing the 15 cm long sandstone column, with each element having a width of 0.005 m; and D 1 representing the inactive element with a specified pressure of 3.0 MPa, which corresponds to the discharge from the column outlet. Figure 3 shows the geometry of the numerical grid corresponding to laboratory test conditions.

Model parameterization and calibration procedure

Multiplication of kinetic constant and specific reactive surface area *k*S values for primary and secondary minerals (Table 2) used as an estimated calibration parameters to fit model output results to laboratory test data observed.

Modeling runs outputs, including transient mineral fractions and chemical concentrations of fluid were printed out at those times corresponding to the sampling times of alkaline fluid discharge from the column outlet (9, 16, 23, 30, 32, 58, and 79 days). At this times comparison of calculated and observed system state made and updating calibration parameters (kS values) performed. Iteration of modeling runs done until no further improvement of the fit obtained.

MODELING RESULTS

Necessity of precipitation\dissolution restrain

Based on a number of initial calibration runs it was not found scenario which show appearance of the new secondary minerals and reducing old one and change of fluid chemical concentrations at the sample site outlet in a way similar to laboratory test performed. Hence some minerals were constrained in the model to precipitate or dissolve according to laboratory test results (see above). Specifically, (1) K-feldspar, albite, chlorite, and muscovite were constrained from precipitation, whereas (2) Na-smectite (montmorillonite), kaolinite and sodium carbonates were prevented from dissolution, e.g. not allowed to dissolve in the model.

Modeling without cation exchange

Seven modeling runs were performed with different kS values, no cation exchange option enforced. The modeling scenario (run #7A) yielded the following results.

Mineral-phase fractions change. Mineral percentage relative to the total amount of secondary minerals used as measure of mineral fractions change. By the end of day 79, in response to alkaline solution injection the most significant dissolution took place at the entry of the column: quartz dissolves most significantly (up to 2156%), muscovite (up to 1470%), microcline (up to 70%), albite (up to 32.5%), while chlorite insignificantly dissolves (up to 0.03%). Calcite

precipitate with maximum 48.8% in the entry part of the column, Na-smectite (montmorillonite) precipitates ranges from 6.8% to 49.5% trending to increase by the column outlet, kaolinite precipitates increase from 1.15% at the entry to 15.8% at the mid part, then drop to 0.3% at the outlet. Total relative volume of secondary minerals generated in column during experiment estimated in the model by range of 0.0005-0.015%, increasing from entry to the column outlet. In general, these results match with laboratory test results, except that no sodium-rich solid mentioned in Table 2 was obtained in the model (whereas abundant sodium carbonates were observed during the laboratory test).

Space distributions of chemical elements in liquid phase and pH along the direction of injected fluid in the column by day 79 of the laboratory test show constant concentration distributions.

Comparisons between observed and modeled transient-chemical-concentration data taken from fluid sampled in the sandstone column outlet (Run #7A) show that the pH follows the same trend in both the model and experiment, whereas absolute modeling values are 2.6 units larger than the measured pH. The model-calculated Na matches the experimental data reasonably well. The Ca comparison between model and experiment shows the same trend, with the absolute values in the model 1 order less than in the experiment. The K values are under-predicted by the model. The Mg comparison shows the same trend between model and experiment, with model absolute values 2–3 orders of magnitude less. The Al comparison shows a model is 4 orders of magnitude greater than experimental values. The Si comparison shows convergence at early times, but later model concentrations are three times greater than in the experiment.

It was also found that a change of rate constants in mineral precipitations (*k*S) for Na-smectite and kaolinite (Table 2) has no effect on the pH and outlet discharge transient chemical concentrations.

Model sensitivity to thermodynamic data

Model sensitivity to assumed solid sodium thermodynamic data tested too. In this way sodium carbonate Na_2CO_3 logK values shifted down, having in a mind some uncertainty of the thermodynamic data used. It was found 4 logK units is a shifting threshold to get solid sodium phase (up to $3.68\ 10^{-3}$) in the inflow part of the model (run #12). Similarly shifting trona thermodynamic logK values on 6 units down makes model able to generate trona ($7.4\ 10^{-4}$ – $1.41\ 10^{-1}$) along all the length of the sample (run #14).

Modeling with cation exchange.

Additional modeling runs (run #15) performed taking into account possible cation exchanges into consideration (Na, K, Ca, Mg, H) (Table 5). This improve model and experimental data convergence: abundant dawsonite precipitation was observed in the model confirm this is the best candidate of sodium carbonates to be precipitate during laboratory test, transient concentrations and pH values at the outlet of the sample column are better reproduced in the model.

Hence, the modeling scenario (run #15) yielded the following results.

Mineral-phase fractions change (Figure 4). Mineral percentage relative to the total amount of secondary minerals used as measure of mineral fractions change. By the end of day 79, in response to alkaline solution injection: calcite dissolves with maximum 13.5% in the mid of the column, quartz dissolves (from 10.0% at the column entry to 0.8% at the outlet), muscovite dissolves (from 6.7% to 0.7%), microcline dissolves (from 0.3% to 0.04%), albite dissolves slightly (from 0.15 to 0.04%), chlorite dissolves insignificantly (less than 0.08%). Na-smectite (montmorillonite) precipitates increase to the outlet part of the column (from 0.002% to 39.8%), kaolinite precipitates increase from 0.05% at the entry up to 10.7% in the mid part of the column, then drop to 2.4% at the outlet. Model shows also significant dawsonite generation ranging from 49.9% at the column entry to 7.8% at the outlet, which correspond to sodium carbonates, observed during laboratory test but not clearly identified on the basis of ESD. Total relative volume of secondary minerals generated in column during experiment estimated in the model by range of 0.1-

0.8%, increasing from entry to column outlet. Modeling shows that after 32 day of the laboratory experiment dawsonite generation stopped (Figure 6).

Although model and experimental data convergence of the transient Na, K, Ca, Mg, Al, Si-concentrations and pH values at the outlet of the sample column improved, but still rather qualitative (Figs. 6-7).

Comparisons between observed and modeled transient-chemical-concentration data taken from fluid sampled in the sandstone column outlet (Run #15) show that the pH converge in "average terms" in the model and experiment, whereas modeling values are 2 units less during first half of experiment time and 2.5 units greater during second half of the experiment time compare to measured pH (Figure 6). The model-calculated Na matches the experimental data reasonably well (Figure 6). The Ca values are over-predicted by the model at the beginning and under-predicted at the end of experiment (Figure 6).

The K comparison between model and experiment shows the same trend, with the absolute values in the model 1 order less than in the experiment. The Mg comparison shows the same trend between model and experiment, with model absolute values 2–3 orders of magnitude less. The Al comparison shows the model and experiment low concentrations during 1-st half of experiment time, which may correspond to Al detection limit, while by day 45 Al and pH breakthrough observed in the model, whereas not detected in experiment. The Si comparison shows convergence at early times, but later model concentrations are 2 orders greater than in the experiment.

Effect of carbonation injected fluid.

Two runs (#16A and 17A) were performed to investigate effect of partial carbonation of injected fluid before injection, that might be because reagent NaOH have absorbed some CO_2 from air before solution was made up, and/or the injection fluid itself might have absorbed some CO_2 prior injection. P_{CO2} assigned 0.1 and 0.2 bars respectively for those runs, but no significant changes in modeling outputs compare to run #15 observed.

CONCLUSIONS

(1) TOUGHREACT V1.0 modeling was used to reproduce laboratory tests on sandstones samples collected from a deep radionuclide repository site in the Siberia Chemical Plant. Laboratory tests included injection of alkaline fluids into sandstones samples at 70^{o}C. Based on laboratory test results, some minerals were not allowed to precipitate or dissolve in the model. Cation exchange option used. Modeling outputs were compared to observed laboratory test data (mineral-phase change and transient concentration data at the outlet of the sample column).

(2) Model and test convergence were obtained in the principal mineral phases (Na-smectite and kaolinite precipitation; quartz, microcline, chlorite and muscovite dissolution). The model generate dawsonite, which correspond to sodium carbonates observed in the laboratory test. Modeling and observed transient chemical concentration data at the outlet of the sample column (Na, K, Ca, Mg, Al, Si and pH) are rather qualitative.

Additional modeling to match laboratory test data ongoing.

ACKNOWLEDGMENTS

We express our gratitude to T. Xu, N. Spycher, and J. Apps (Lawrence Berkeley National Laboratory) for valuable comments and suggestions, as well as B.N. Ryzhenko and O.A. Limantseva (GeoChi RAS), and I.B. Slovtsov (IVS FEB RAS) for additional thermodynamic calculations. Special thanks to A.A. Grafchikov, Institute of Experimental Mineralogy RAS, who provided microprobe analysis data. Authors appreciate useful Reviewers comments. This study was supported by FEB RAS Project 06-I-OH3-109 and RFBR Project 06-05-64688-a.

REFERENCES

1. Kamnev, E.N., and A.I. Rybalchenko, Deep injection of liquid radioactive waste in cuclear industry enterprises. *Engineering Ecology*, 1, 2–9 (in Russian), 2001.

2. Okunkov, G.A., Rybalchenko A.I., and Kuvaev A.A., Heat regime of the geological repository site caused by liquid radionuclide waste injection. *Geoecology*, 3, 237–244 (in Russian), 2003.

3. Rybalchenko A.I., Pimenov M.K., Kostin P.P. et al., Deep injection of liquid radionuclide waste. *IzdAT*, Moscow, 256 p. (in Russian), 1994.

4. Zubkov A.A., Makarova O.V., Danilov V.V., Zakharova E.V., Kaymin E.P., Menyailo K.A., and Rybalchenko A.I., Technogenic geochemical processes during injection of liquid radionuclide waste into sandstone layer-type reservoirs. *Geoecology, Engineering Geology, Hydrogeology, Geocriology*, 2, 133–144 (in Russian) 2002.

5. Kaymin, E.P., E.V. Zakharova, L.I. Konstantinova, A.A. Graphchikov, L.Y. Aranovich, and V.M. Shmonov, Study of the interaction of alkaline radionuclide waste with sandstone rocks. *Geoecology, Engineering Geology, Hydrogeology, Geocriology*, 5, 427–432 (in Russian), 2004.

6. Xu, T., Sonnenthal E., Spycher N. TOUGHREACT User's Guide: A Simulation Program for Nonisothermal Multiphase Reactive Geochemical Transport in Variably Saturated Geologic Media \\ LBNL-55460, 2005, 192 p.

7. Kiryukhin, A.V. T. Xu, K. Pruess, J. Apps, and I. Slovtsov, Thermal-hydrodynamic-chemical (THC) modeling based on geothermal field data. *Geothermics,* 33(3), 349–381, 2004.

8. Kiryukhin, A.V., Puzankov M.Y., Slovtsov I.B., Bortnikova S.B., Moscaleva S.V., Zelensky M.E., and Polyakov A.Y Thermal-hydrodynamic-chemical modeling processes of secondary mineral precipitation in production zones of geothermal fields. *Vulcanologia and Seismologia*, 5, 27-41, (in Russian), 2006.

9. Chapovsky E.G. Laboratory studies in soils mechanics, Moscow, Gosgeoltechisdat, 1958, 272 p. (in Russian).

10. Grafchikov A.A., Aranovich L.Ya., Shmonov V.M., Zakirov I.V., Kaymin E.P., Zakharova E.V. Experimental simulation of sandstone interaction with Na-bearing alkalie solution in a flow regime // *Geochemistry*, 2004, #6, p. 632-647 (in Russian).

11. Grafchikov A.A., Aranovich L.Ya., Shmonov V.M., Zakirov I.V., Kaymin E.P., Zakharova E.V. Experimental simulation of sandstone interaction with Na-bearing alkaline solution in a flow regime// *Geochemistry International* , v.42, №6, p.545-560, 2004.

Table 1. Initial mineral fractions observed in the sample and assumed in the modeling (run #7A).

Mineral Phase (Observed)	Weight %	Mineral Phase (assumed in the modeling)	Vol. % (run#7)
Qtz—quartz	50	Quartz	50
Kfs—K-feldspar	10	Microcline	10
Mont—montmorillonite	10	Na-smectite	10
Kaol—kaolinite	10	Kaolinite	10
Ab—albite	5	Albite (low)	5
Chl—chlorite	3	Chlorite	3
h-Bt—hydrated biotite, Mont-Bt—mont. biotite	5		
Ms—muscovite, Mont-Ms—mont. muscovite	2	Muscovite	11
Sid—siderite	2		
Cc—calcite	<1	Calcite	1
Ap—apathite, Ilm—ilmenite	<1		
		Sodium carbonates: Natrite Na_2CO_3	0
		Trona $Na_3CO_3\ HCO_3 2H_2O$	0
		Dawsonite $NaAlCO_3(OH)_2$	0

Table 2. Parameters for chemical interaction of mineral phases (run #7A): E_a – activation energy [7], kJ/kmol, *k*S - multiplication of *k,* kinetic constant of the mineral dissolution/precipitation at 25 C, mole/s·m^2 and S, specific reactive surface area, m^2/m^3.

Note: *k*S used as a calibration parameter in the model.

Mineral Phase	E_a, kJ/mol	Dissolution kS mol/s m^3	Precipitation kS mol/s m^3
Quartz	75.00	1.0e-8	1.0e-8
Microcline	67.83	1.0e-9	0.0
Na-smectite	58.62	0.0	1.0e-2
Kaolinite	62.76	0.0	1.0e-2
Albite (low)	67.83	1.0e-9	0.0
Chlorite	58.62	1.0e-9	0.0
Muscovite	75.0	1.0e-9	0.0
Sodium carbonates: Natrite Na_2CO_3	62.76	0.0	1.0e-2
Trona Na_3CO_3 $HCO_3 2H_2O$	62.76	0.0	1.0e-2
Dawsonite $NaAlCO_3(OH)_2$	62.76	0.0	1.0e-2

Table 3. The initial pore-fluid and injected-fluid chemical composition as analyzed and assigned in the model. The chemical composition of injected fluid was calculated based on the following initial concentrations (g/L): $NaNO_3$ = 44.3; Na_2CO_3 = 2.08; Al = 0.83, NaOH = 8.9. Chemical composition was converted to the primary species concentrations mol/kg H_2O; pH = 11.67 (as estimated by I.B. Slovtsov, using Selector software) = 11.67, and pH= 11.81 (as estimated by O.A. Limantseva, using Gibbs software).

Primary species	Initial Pore Fluid			Injected Fluid	
	Chemical Analysis	Assigned in the TOUGHREACT modeling			
pH	7.3	7.3		11.81	
	mg/L	mg/L	mol/kgH_2O	mg/L	mol/kg$_{H2O}$
Na^+	26.30	26.30	1.143976E-03	17570	0.764
K^+	2.90	2.90	7.417259E-05		0.1E-06
Ca^{++}	25.00	25.00	6.237836E-04		0.1E-06
Mg^{++}	15.30	15.30	6.295001E-04		0.1E-06
Fe^{++}	5.80	5.80	1.038589E-04		1.0E-15
AlO_2^-	0.00		0.10000E-07	1810	0.030
Cl^-	7.10	7.10	2.002651E-04		0.1E-06

SO_4^{--}	3.20	3.20	3.331113E-05		0.1E-06
HCO_3^-	230.00	230.00	3.769441E-03	1220	0.020
NO_3^-			0.10000E-06	32300	0.521
SiO_2(aq)			0.10000E-06		0.1E-06

Table 4. Initial fluid chemical composition and transient data on chemical composition from fluid sampling at the column outlet

Time, days	Volume of injection, ml	pH	Concentration, ppm						
			Na	Al	Si	Ca	Mg	K	Sr
Initial fluid		11.8	17300	955	<0.5	<0.1	<0.01	7.95	<0.01
9	12.5	7.55	12100	≤0.1	47.1	1140	106	85.1	86.9
16	11	8.78	15300	≤0.1	30.6	14.7	11.7	73.8	3.92
23	10.2	8.98	15100	≤0.1	42.4	8.92	7.92	68.9	2.16
30	10	8.84	15500	≤0.1	42.4	6.4	4.24	65.9	1.42
32	12	8.20	17000	≤0.1	40.0	2.5	2.03	57.1	1.35
58	31.5	8.92	17500	≤0.1	1.58	1.46	0.65	44.5	0.29
79	30.5	8.85	17500	≤0.1	2.13	2.32	0.84	64.3	0.34

Table 5. Cation exchange parameters used in the modeling scenario #15, cation exchange capacity 6.5 meq/100 g of solid used.

Cation	Exchange coefficient
Na^+	1.0
K^+	0.1995
Ca^{++}	0.3981
Mg^{++}	0.5012
H^+	1.0e-09

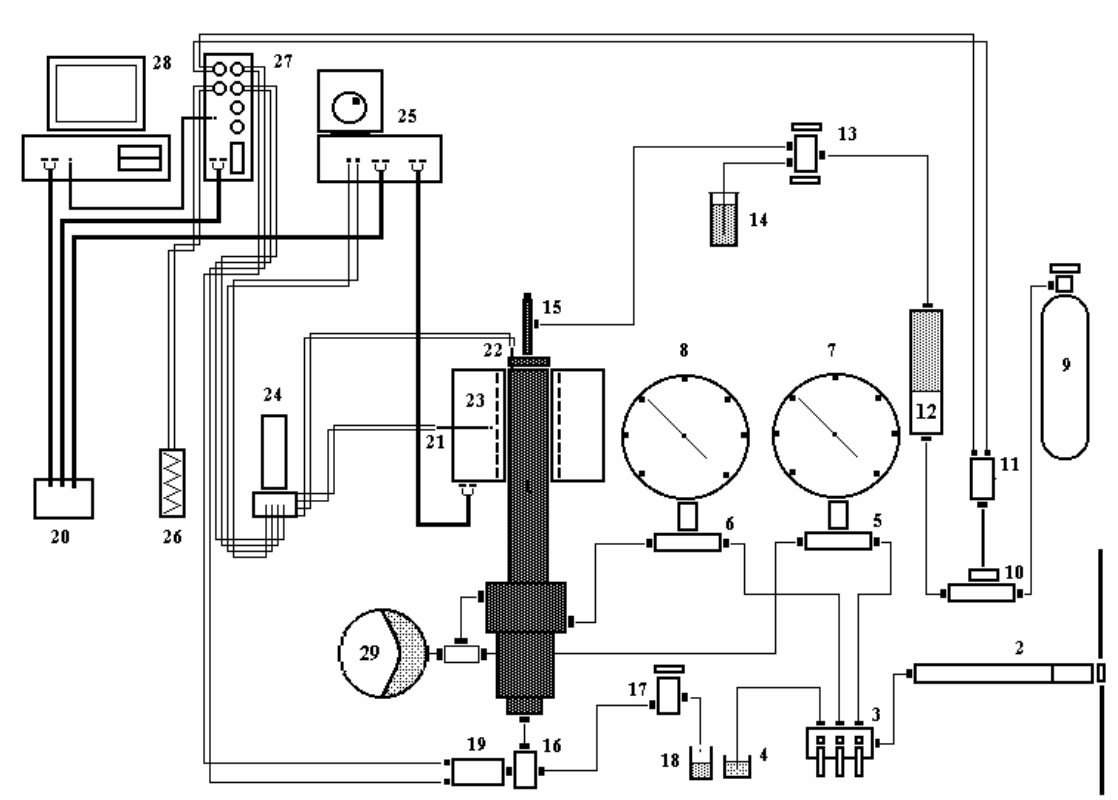

Figure 1. Laboratory experiment setup: 1 - High pressure vessel (rock sample site), 2 - Screw press, 3 - Triple valve, 4 - Vessel with water, 5,6 - Pressure gauges set, 7,8 - Pressure gauges, 9 - Gas vessel, 10 - Pressure gauge set, 11 - Pressure gauge, 12 – Separator, 13 - Double valve, 14 - Vessel with solution, 15 - Input nozzle, 16 - Triple valve, 17 - Output solution valve, 18 - Output solution vessel, 19- Pressure gauge, 20 - EC distributor, 21, 22 – Thermocouples, 23 - Electrical heater, 24 - Cold alloy thermostat, 25 - Temperature regulator, 26 - Thermo-resistor, 27 - Parameters registration block, 28 – PC, 29 - Environmental temperature and pressure compensator.

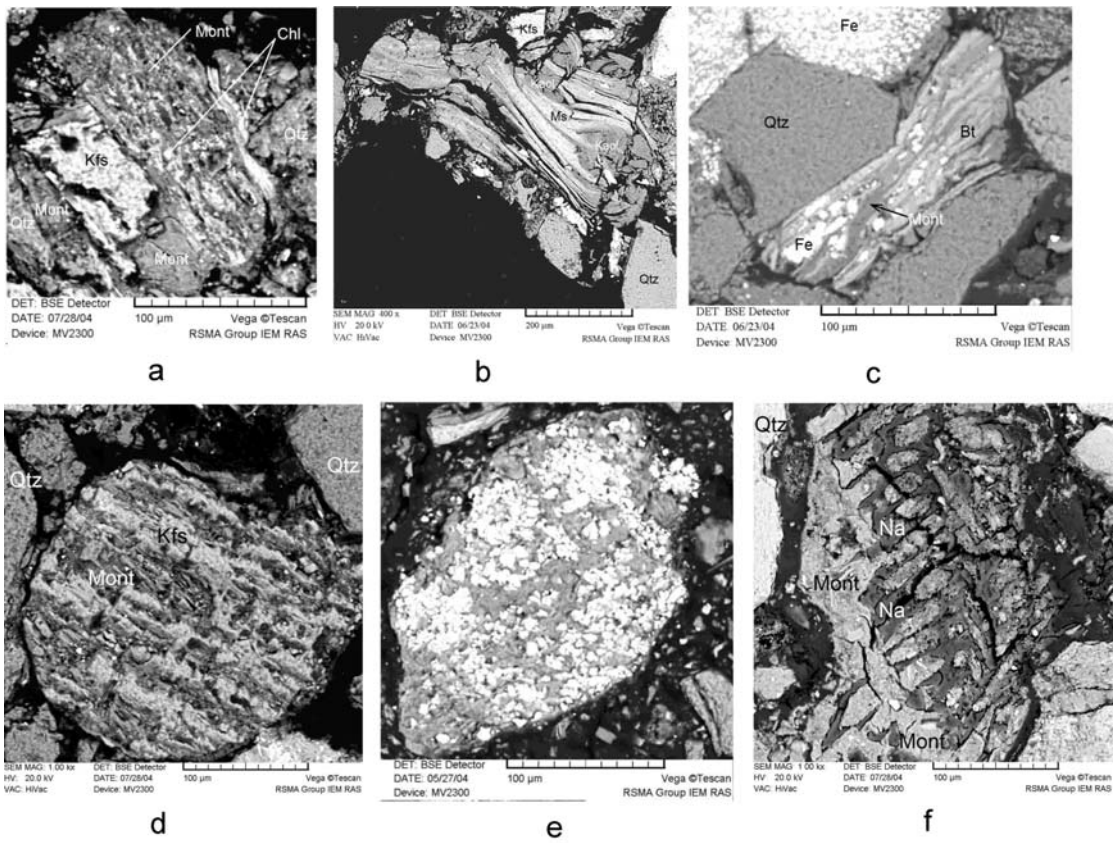

Figure 2. Electron-scan images of samples (E.P. Kaymin data) after laboratory test: (a) chlorite (Chl) replacement by montmorillonite (Mont); (b) muscovite (Ms) replacement by kaolinite (Kaol); (c) biotite (Bt) replacement by montmorillonite (Mont); (d) K-feldspar (Kfs) replacement by montmorillonite (Mont); (e) grains of magnetite hosted in clay minerals; (f) sodium carbonates (Na) release in form of regions in montmorillonite (Mont). The black space is the polymeric matrix.

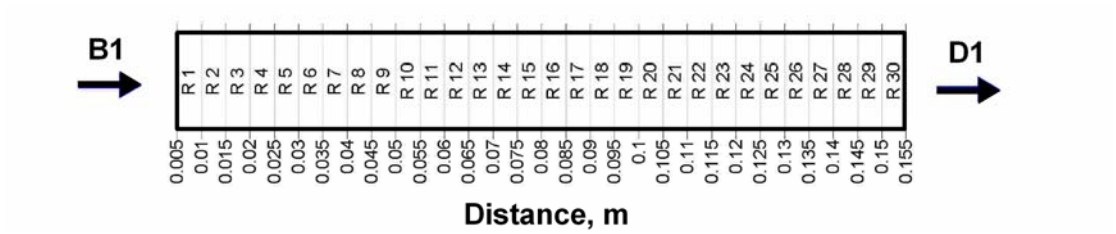

Figure 3. Numerical grid geometry used for modeling alkaline $NaNO_3$-NaOH fluid injection in a sandstone column from the SCP deep repository site. B1 – injection element, D1 – discharge element.

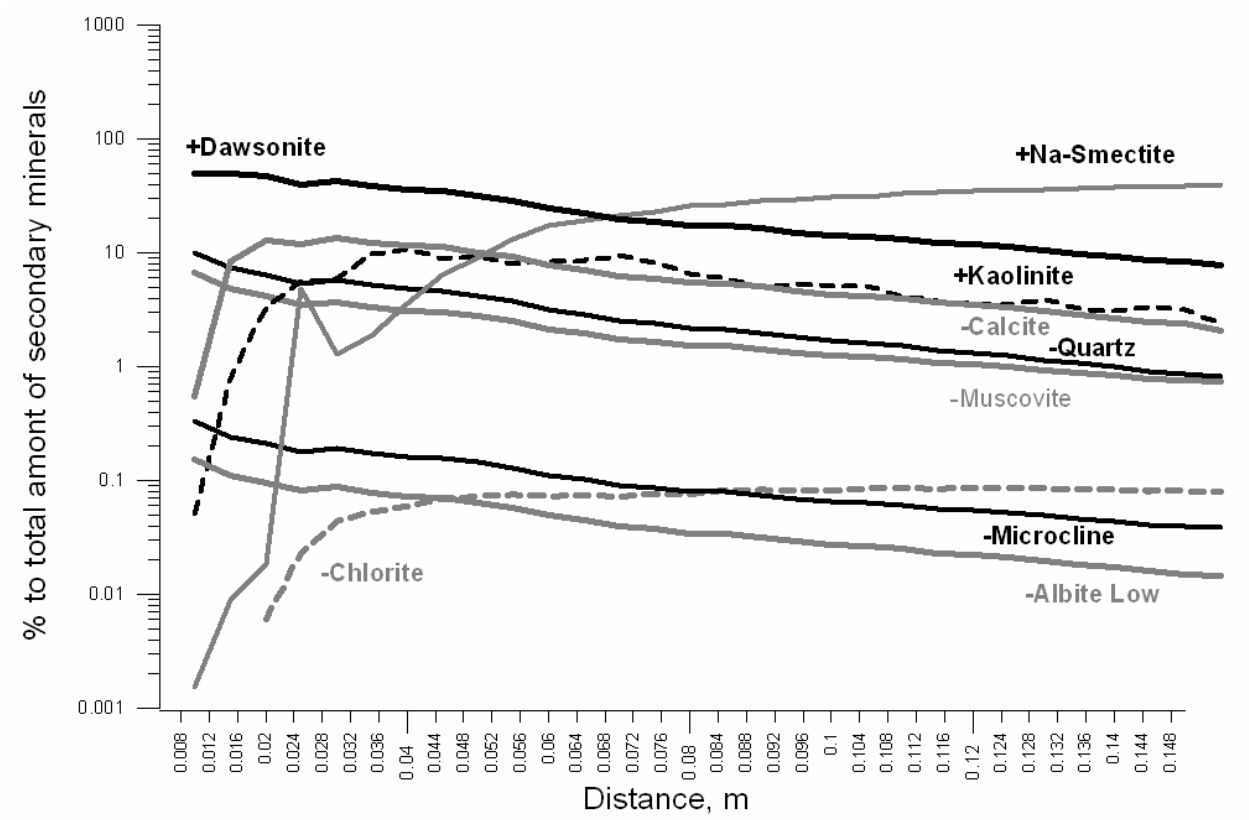

Figure 4. Modeling results (run #15, cation exchange option enforced). Mineral percentage relative to the total amount of secondary minerals along the injection direction within the sandstone column sample by 79 days of modeling time. Mineral percentage values are represented in log scale, precipitated phases are denoted with a (+) symbol, whereas dissolved phases are denoted with a (-) symbol.

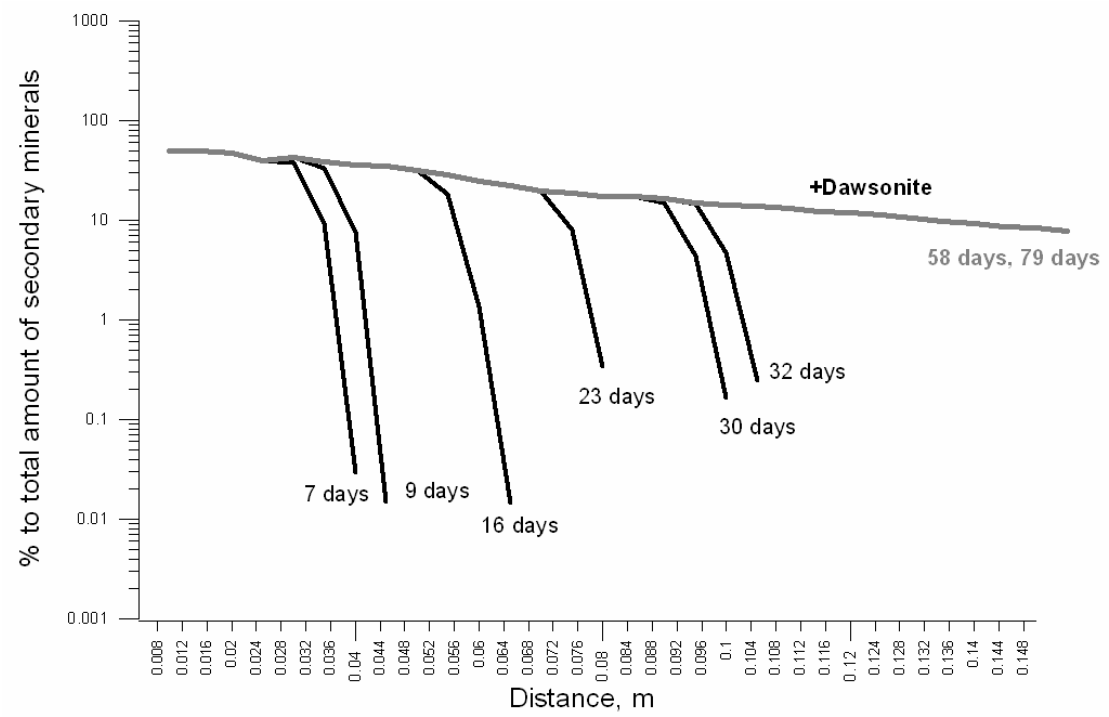

Figure5. Modeling results (run #15, cation exchange option enforced). Mineral percentage of dawsonite relative to the total amount of secondary minerals along the injection direction within the sandstone column sample at different modeling times.

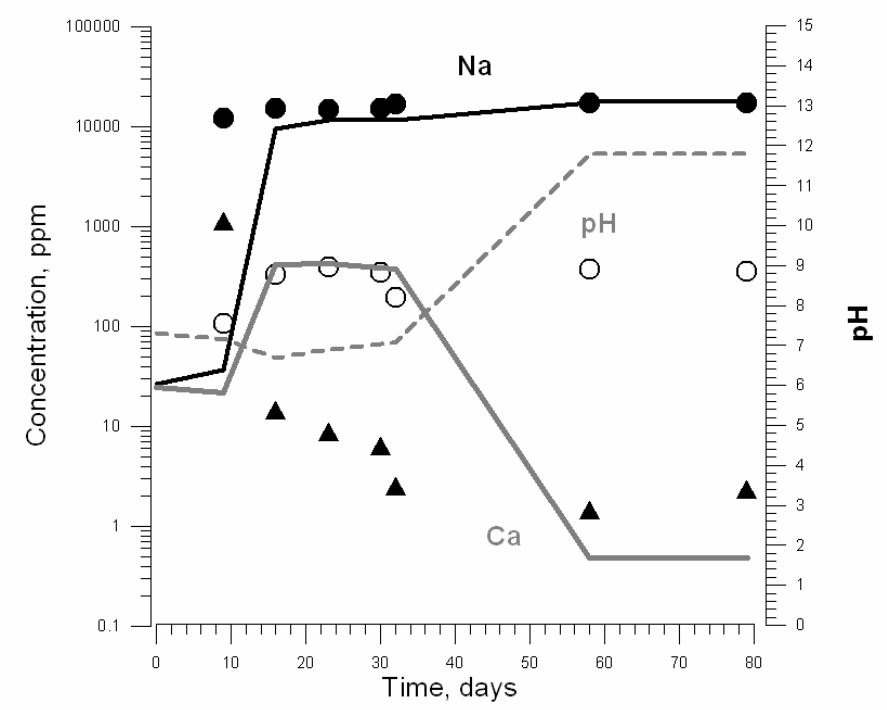

Figure 6. Comparison of the modeling results (lines, run #15, cation exchange option enforced) and transient pH data (empty circles), Na-concentrations data (filled circles) and Ca-concentrations data (triangles) at the outlet of the sample site during laboratory test.